ChemComm

Construction of α-helical peptide dendrimers conjugated with multi-metalloporphyrins: photoinduced electron transfer on dendrimer architecture

Muneyoshi Sakamoto, Akihiko Ueno and Hisakazu Mihara*

Department of Bioengineering, Graduate School of Bioscience and Biotechnology, Tokyo Institute of Technology, Nagatsuta, Yokohama 226-8501, Japan. E-mail: hmihara@bio.titech.ac.jp

Received (in Cambridge, UK) 11th May 2000, Accepted 31st July 2000
First published as an Advance Article on the web 25th August 2000

Noncovalent assembly of Zn^{II}–mesoporphyrin IX was accomplished by coordination to α-helical peptides (4–64 segments) based on polyamideamine dendrimer; the electron transfer functions were expressed more effectively with the growth of the dendrimer generation.

Assemblies of peptides or functional groups perform a significant role in nature, displaying highly efficient functions including energy transfer and electron transfer. For example, in photosynthetic bacteria, light-harvesting complexes (LH),[1] in which many bacteriochlorophylls are assembled and oriented with α-helix peptides, absorb light energy, and delocalize and transfer the energy to the reaction center where charge separation occurs. The development of an artificial system with native-like properties but without the complexity of the natural components, has been attempted using *de novo* designed peptides.[2,3] On the other hand, dendrimers have also attracted much attention in the field of polymer chemistry.[4–8] Some dendrimers have been investigated for electron transfer[6] and energy transfer[7] functions because of their morphological similarities to LH. Using dendrimers as templates in the *de novo* design proteins, the peptide assembly conditions and functionalization may be controlled precisely. In this study, designed amphiphilic α-helix peptides (4, 8, 16, 32 and 64 segments) were introduced at the end groups of polyamideamine dendrimers (PAMAMs)[4] (Fig. 1). Zn^{II}–Mesoporphyrin (Zn-MP) was coordinated between the 2α-helix peptides[3] to accomplish a multi-Zn-MP array so that electron transfer properties were expressed more effectively with the growth of the dendrimer generation.

Synthesis of peptide dendrimers was performed by a domain ligation strategy.[8] The 20-residual peptide (R-HL4) was designed to take an amphiphilic α-helical structure, which was stabilized by four sets of Glu–Lys salt bridges. As an axial ligand of metalloporphyrin, His was introduced to deploy a porphyrin parallel to the helix axis. Four Leu residues per α-helix were arranged to construct a hydrophobic pocket as a porphyrin-binding site.[3] Cys was used at the N-terminus of the peptide to ligate to the outer termini of the template dendrimer through the thioether linkage. Arg was introduced at the C-terminus of the peptide to form an electrostatic field at the outer shell of the peptide dendrimers. R-HL4 was synthesized by the solid-phase method using Fmoc-strategy and purified with reversed-phase (RP) HPLC. The peptide was identified by matrix assisted laser desorption ionization time-of-flight mass spectrometry (MALDI-TOFMS).[9] To conjugate the peptide with PAMAM [Starburst Dendrimer, G0, G1, G2, G3 and G4, from Aldrich], the chloroacetyl group was introduced at each amino terminal group of PAMAM, by treatment with *N*-ethoxycarbonyl-2-ethoxy-1,2-dihydroquinoline[10] and chloroacetic acid in MeOH. Perchloroacetylated (*n*-ClAc) PAMAMs were purified by size exclusion chromatography (SEC, Sephadex LH-60–MeOH) and RP-HPLC, and identified by MALDI-TOFMS.[11] R-HL4 and *n*-ClAc-PAMAM were combined by the ligation reaction[12] between the thiol side chain of Cys in R-HL4 and the chloroacetyl group of *n*-ClAc-PAMAM. The peptide dendrimers, *n*-(R-HL4)PAMAMs, were purified by SEC (Sephadex G-50–30% AcOH) and RP-HPLC, and identified by MALDI-TOFMS[13] or ultracentrifugation.[14]

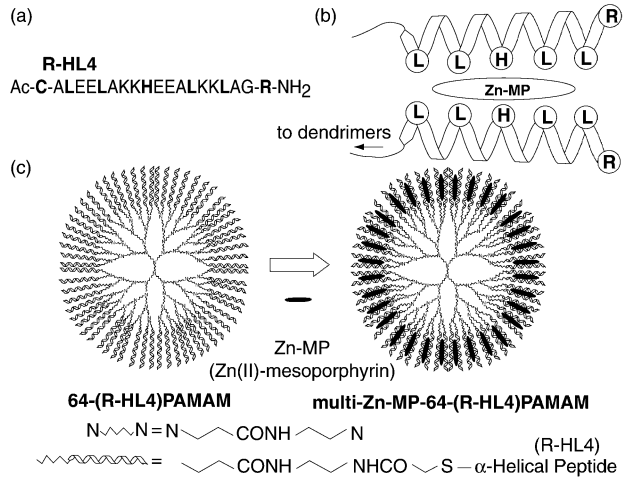

Fig. 1 Structure of the peptide dendrimers, (a) amino acid sequence of R-HL4; (b) schematic illustration of Zn-MP coordination to 2α-helix; and (c) 64-(R-HL4)PAMAM and multi-Zn-MP-64-(R-HL4)PAMAM.

Circular dichroism (CD) study revealed that *n*-(R-HL4)PAMAM, (*n* = 4, 8, 16, 32 and 64) showed a typical α-helical pattern in pH 7.4 buffer. The α-helicity[15] of the peptides in the dendrimers was estimated as *ca*. 50% (Table 1), indicating that *n*-(R-HL4)PAMAMs with different extents of dendrimer generation have similar α-helical properties. UV-Vis titration[3] of Zn-MP with *n*-(R-HL4)PAMAM showed an increase of the Soret band at 415 nm and decrease of the band at 403 nm of Zn-MP. The binding constant (K_a) was determined from the absorbance change at 415 nm using an equation assuming the 1/*n* (2α-helix in peptide dendrimer–Zn-MP) complexation (Table 1). The *n* values were found to be close to 1.0, indicating that Zn-MP bound to the peptide dendrimers almost equivalently per 2α-helix. The K_a values indicated that Zn-MP bound to the peptide dendrimers efficiently, and binding affinities to peptide dendrimers were almost identical. *n*-(R-HL4)PAMAM conjugated with multi-Zn-MP showed a strong induced CD

Table 1 Ellipticity at 222 nm and α-helicity of peptide dendrimers, and binding constant K_a and *n* value for peptide dendrimers with Zn-MP

n-(R-HL4) PAMAM	$[\theta]_{222}/10^4$ deg cm^2 dmol^{-1}	α-Helicity (%)	$K_a/10^5$ dm^3 mol^{-1}	*n* value
n = 4	−1.68	53	3.2	1.01
n = 8	−1.67	53	1.7	0.84
n = 16	−1.51	48	1.5	0.93
n = 32	−1.45	46	1.8	0.98
n = 64	−1.45	46	2.1	0.99

Ellipticity [θ] at 222 nm and α-helicity were estimated from the CD spectra. [*n*-(R-HL4)PAMAM] = 1.0×10^{-5} mol dm^{-3} (per 2α-helix), in 2.0×10^{-2} mol dm^{-3} Tris·HCl buffer (pH 7.4) at 25 °C. The binding constant K_a and *n* value were estimated by UV-Vis spectra titration, in pH 7.4 buffer at 25 °C. [Zn-MP] = 5.0×10^{-6} mol dm^{-3}.

DOI: 10.1039/b003786i

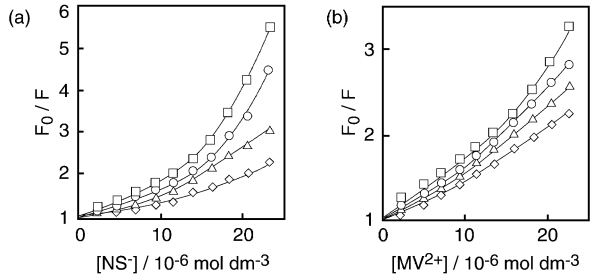

Fig. 2 Stern–Volmer plot for fluorescence quenching of Zn-MP (2.5×10^{-7} mol dm^{-3}) conjugated with *n*-(R-HL4)PAMAM (7.5×10^{-7} mol·dm^{-3} per 2α-helix) by quenchers. λ_{ex} = 415 nm, λ_{em} = 582 nm, in the buffer (pH. 7.4) at 25 °C. Electron acceptors = (a); NS^-, (b); MV^{2+}: □; *n* = 64, ○; *n* = 32, △; *n* = 16, ◇; *n* = 8 and 4.

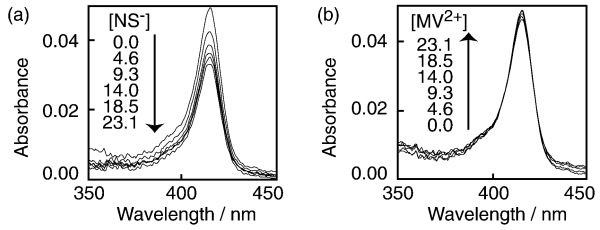

Fig. 3 UV-Vis spectra of Zn-MP (2.5×10^{-7} mol dm^{-3}) conjugated with 64-(R-HL4)PAMAM (7.5×10^{-7} mol dm^{-3} per 2α-helix) with increasing concentration (0, 4.6, 9.3, 14.0, 18.5, 23.1 $\times 10^{-6}$ mol dm^{-3}) of electron acceptors, (a); NS^-, (b); MV^{2+} in the buffer (pH. 7.4) at 25 °C.

peak at the Soret region,[16] suggesting that Zn-MP was coordinated in a regulated manner. In addition, the α-helicity was not changed by the binding with Zn-MP.

To examine electron transfer properties of multi-Zn-MP-conjugated *n*-(R-HL4)PAMAM, fluorescence quenching studies were performed by the addition of a negatively charged electron acceptor, naphthalene sulfonate[6] (NS^-), and a positively charged methylviologen[6] (MV^{2+}). Upon excitation at the Soret band, multi-Zn-MP–*n*-(R-HL4)PAMAM emitted fluorescence at 582 and 630 nm, which was quenched by the addition of NS^-. The Stern–Volmer plots (Fig. 2a) showed that the quenching occurred more strongly with increase in dendrimer generation. In each generation, the concentrations of 2α-helix and Zn-MP were constant. This result indicates that the positive charges of Arg residues were assembled more densely on the surface of the peptide dendrimer with the growth of each generation so that the negative charged NS^- was bound more effectively by the electrostatic force. Consequently, quenching was amplified with the growth of generation. On the other hand, when positively charged MV^{2+} was employed, the fluorescence quenching (Fig. 2b) was also observed to increase with the growth of the peptide dendrimer, although the charge repulsion became stronger with the generation growth. It was suggested that the quenching mechanism of MV^{2+} was different from that of NS^-. To examine these mechanisms, UV-Vis spectra on the addition of NS^- and MV^{2+} were measured (Fig. 3). In the case of NS^-, the Soret band decreased, supporting electrostatic binding between multi-Zn-MP–*n*-(R-HL4)PAMAM and NS^- in the ground state. By contrast, UV-Vis spectra were little changed by the addition of MV^{2+}, indicating that MV^{2+} does not have a strong influence on the ground state of Zn-MP. Table 2 shows the fluorescence lifetimes of multi-Zn-MP–*n*-(R-HL4)PAMAM. With the growth of generation, a percentage of the long-lived component (2.3–2.6 ns) increased. In 32- and 64-(R-HL4)PAMAM, the short-lived component (1.7–1.8 ns) disappeared. In the presence of NS^-, the fluorescence lifetime of multi-Zn-MP–64-(R-HL4)PAMAM was not changed (2.3 ns). This result supports the idea that NS^- causes electron transfer by a static mechanism.[17] By contrast, addition of MV^{2+} caused the fluorescence lifetime to be extremely shortened (0.5 ns, 88%). These results indicated that the electron was transferred mainly by a dynamic mechanism.[17]

Table 2 Fluorescence lifetime of multi-Zn-MP–*n*-(R-HL4)PAMAM

n-(R-HL4) PAMAM	Electron acceptors	τ_1/ns	A_1 (%)	τ_2/ns	A_2 (%)
n = 4	—	1.8	74.7	2.6	25.3
n = 8	—	1.8	73.8	2.6	26.2
n = 16	—	1.7	47.8	2.3	52.2
n = 32	—	—	—	2.4	100.0
n = 64	—	—	—	2.3	100.0
n = 64	NS^-	—	—	2.3	100.0
n = 64	MV^{2+}	0.5	88.0	2.3	12.0

Fluorescence lifetime was measured using Zn-MP (2.5×10^{-7} mol dm^{-3}) conjugated with *n*-(R-HL4)PAMAM (7.5×10^{-7} mol dm^{-3} per 2α-helix) at 25 °C. λ_{ex} = 415 nm, λ_{em} = 570–650 nm, electron acceptors, [NS^-] = [MV^{2+}] = 2.0×10^{-5} mol dm^{-3}. Decay profiles were analyzed by the double exponential equation, $I_f(t) = A_1\exp(t/\tau_1) + A_2\exp(t/\tau_2)$.

In conclusion, noncovalent Zn-MP assembly was accomplished by coordination to novel peptide dendrimers, and the electron transfer function was expressed more effectively with the growth of dendrimer generation. Dynamic quenching with viologen can be applied to the catalytic reactions. The nanoscale assembly of a system combining *de novo* designed peptides with dendrimers will be utilized in artificial photosynthesis.

We are grateful to Dr K. Aoi, Nagoya University, for valuable discussions on dendrimers, Dr F. Arisaka, Tokyo Institute of Technology, for ultracentrifugation analyses and Dr S. Sakamoto, Tokyo Institute of Technology, for valuable discussions on the *de novo* design.

Notes and references

1 G. McDermott, S. M. Prince, A. A. Freer, A. M. Hawthornthwaite-Lawless, M. Z. Papiz, R. J. Cogdell and N. W. Isaacs, *Nature*, 1995, **374**, 517.
2 F. Rabanal, W. F. DeGrado and P. L. Dutton, *J. Am. Chem. Soc.*, 1996, **118**, 473; H. K. Rau and W. Haehnel, *J. Am. Chem. Soc.*, 1998, **120**, 468.
3 S. Sakamoto, I. Obataya, A. Ueno and H. Mihara, *J. Chem. Soc., Perkin Trans. 2.*, 1999, 2059; I. Obataya, S. Sakamoto, A. Ueno and H. Mihara, *Protein Peptide Lett.*, 1999, **6**, 141.
4 D. A. Tomalia, A. M. Naylor and W. A. Goddard III, *Angew. Chem., Int. Ed. Engl.*, 1990, **29**, 138.
5 J. F. G. A. Jansen, E. M. M. Branander-van den Berg and E. W. Meijer, *Science*, 1994, **266**, 1226; K. Aoi, K. Itoh and M. Okada, *Macromolecules*, 1995, **28**, 5391.
6 R. Sadamoto, N. Tomioka and T. Aida, *J. Am. Chem. Soc.*, 1996, **118**, 3978.
7 V. Balzani, S. Campagna, G. Denti, A. Juris, S. Serroni and M. Venturi, *Acc. Chem. Res.*, 1998, **31**, 26.
8 C. Rao and J. P. Tam, *J. Am. Chem. Soc.*, 1994, **116**, 6975.
9 MALDI-TOFMS result of R-HL4; 2281.6[(M + H)$^+$] (calc. 2279.7).
10 E. Gross and J. Meienhofer, *The Peptide*, Academic Press, New York, 1979, vol. 1, 289.
11 MALDI-TOFMS data of *n*-(ClAc)PAMAM, *n* = 4; 823.6[(M + H)$^+$] (calc. 823.6): *n* = 8; 2065.7[(M + Na)$^+$] (calc. 2064.7): *n* = 16; 4483.0[(M + H)$^+$] (calc. 4480.9): *n* = 32; 9355.3[(M + H)$^+$] (calc. 9357.4): *n* = 64; 19130.6[(M + Na)$^+$] (calc. 19133.7).
12 S. Futaki, M. Aoki, M. Fukuda, F. Kondo, M. Niwa, K. Kitagawa and Y. Nakaya, *Tetrahedron Lett.*, 1997, **38**, 7071.
13 MALDI-TOFMS data of *n*-(R-HL4) PAMAM (*n* = 4, 8), *n* = 4; 9791.6 [(M + H)$^+$] (calc. 9792.9): *n* = 8; 19900.9[(M + H)$^+$] (calc. 19895.6).
14 *n*-(R-HL4)PAMAMs (*n* > 8) were identified by ultracentrifugation since it was difficult to estimate by MALDI-TOFMS, *n* = 8; found 19900 ± 2100 (calc. 19896): *n* = 16; found 37500 ± 2300 (calc. 40356): *n* = 32; found 84800 ± 7700 (calc. 81108): *n* = 64; found 155100 ± 5700 (calc. 162612).
15 J. M. Scholtz, H. Qian, E. J. York, J. M. Stewart and R. L. Baldwin, *Biopolymers*, 1991, **31**, 1463.
16 CD data at the Soret region of multi-Zn-MP-*n*-(R-HL4)PAMAMs, $[\theta]_{mp}/10^4$ deg cm^2 dmol^{-1} (λ/nm), *n* = 4; +10.3 (413), −9.2 (423): *n* = 8; +7.9 (414), −0.2 (423): *n* = 16; +8.4 (413): *n* = 32, +7.6 (413), −0.2 (423): *n* = 64; +9.7 (413), −0.3 (423).
17 Q. Zhou and T. M. Swager, *J. Am. Chem. Soc.*, 1995, **117**, 12 593.